

## Analysis of Ion Charge States in Solar Wind and CMEs

Arati Dasgupta\* & J. M. Laming

Naval Research Laboratory, Washington DC 20375, USA.

\*e-mail: arati.dasgupta@nrl.navy.mil

**Abstract.** We discuss needs in dielectronic recombination data motivated by recent work directed at a quantitative understanding of ion charge states of various elements observed *in situ* in the solar wind and CMEs. The competing processes of ionization and recombination lead to departures from collision ionization equilibrium. The use of this as a diagnostic of acceleration and heating processes of the solar wind and CMEs is sensitive to the accuracy of the atomic rates in a way that steady state ionization equilibrium plasmas are not. The most pressing need is dielectronic recombination rates for ions Fe<sup>8+–12+</sup>. These are among the dominant species observed in various regions of the solar wind and CMEs, and in remotely sensed EUV spectra.

**Key words.** Solar wind and CMEs—Fe ion charge states—dielectronic recombination.

### 1. Introduction

Interpretation of ion charge states observed *in situ* in the solar wind and also in the CMEs depends on fundamental atomic data for ionization and recombination processes. Determination of dielectronic recombination (DR) data is arguably the most complex and is plagued with most uncertainties for many-electron ions such as M-shell ions of Fe. However, there is an urgent need to determine the DR rate coefficients for these ions, especially the ions of Fe<sup>8+–Fe<sup>12+</sup> and Fe<sup>14+</sup>. These are arguably the most important minor ions in solar physics, having as they do strong emission lines in the extreme ultraviolet (the bandpasses of EIS; the Extreme Ultraviolet Imaging Spectrometer, on Solar-B/Hinode were chosen to maximize the coverage of these lines), and being also the dominant charge states of Fe observed in the fast and slow solar wind. In recent years, a significant world-wide effort has revised the rate coefficients for dielectronic recombination now for all L-shell ions of all elements up to Zn, and a few beyond. For Fe, this means charge states Fe<sup>16+</sup> and up. These data are now incorporated into the most recent computation of steady state ionization balance. Non-equilibrium ionization balance distributions of charge states observed in various regions of the solar wind and CMEs, are considerably less forgiving of inaccuracies in the ionization and recombination rates than are cases where ionization equilibrium can be assumed.</sup>

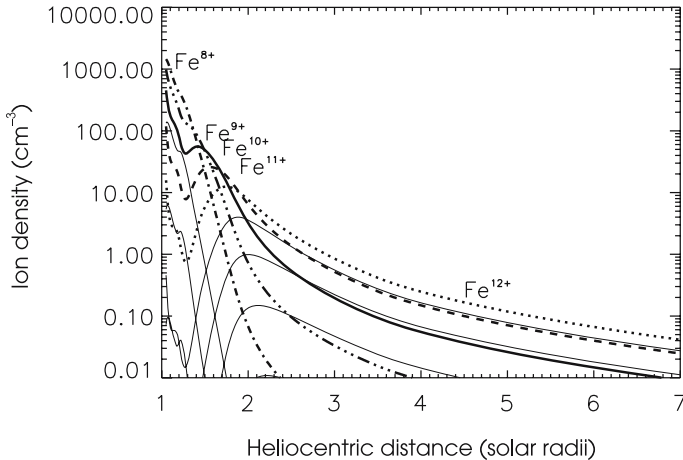


**Figure 1.** Plots of the evolution of the Si and Fe ion charge state densities with heliocentric distance for initial flow speed at 1.05 solar radius  $\text{km s}^{-1}$ . The initial ionization balance corresponds to the coronal hole electron temperature of  $9 \times 10^5 \text{ K}$ . Increased ionization starts at about 1.5 solar radius, as ion-electron energy transfer increases in response to the strong ion cyclotron heating at this location. Charge states are frozen in beyond a distance of 2–2.5 solar radius, and correspond to those measured *in situ* by Ulysses.

## 2. Ion charge states in the solar wind: Modeling approach

The modeling of solar wind charge states generally follows the behavior of the ionization balance of a Lagrangian plasma packet, using an analytic prescription for the hydrodynamic or magnetohydrodynamic evolution. In the case of the fast solar wind, this evolution has been very well studied for polar coronal holes at solar minimum (see Laming 2004 and references therein). For halo CMEs, from which ions are detected *in situ*, we have to make use of observed or modeled height time relations for CMEs propagating across our line of sight. This situation will change with the advent of the STEREO mission. At optimum spacecraft separation, we will be able to observe directly the expansion of a CME from one spacecraft, while the CME plasma is detected at the other. Figures 1 and 2 show the evolution of Si and Fe ion charge state densities. These ion densities were obtained by solving rate equations containing electron impact ionization, radiative and dielectronic recombination rates for each charge states. These rates are the same as those used in the recent ionization balance calculations of Mazzotta *et al.* (1998), with the various updates. Dielectronic recombination from H- to He-like and from He- to Li-like are taken from Dasgupta & Whitney (2004) and DR rates for other ions were obtained from various other sources.

## 3. Atomic physics and ionization balance

Ionization and recombination cross sections and rates can be calculated in the Distorted Wave (DW) or Close-Coupling (CC) approximations. The DW approximation is essentially perturbation theory, and is an excellent approximation for highly charged ions, since the perturbation produced by the scattering electron is small compared to the potential acting on the target electrons due to the nuclear charge. The second approach,

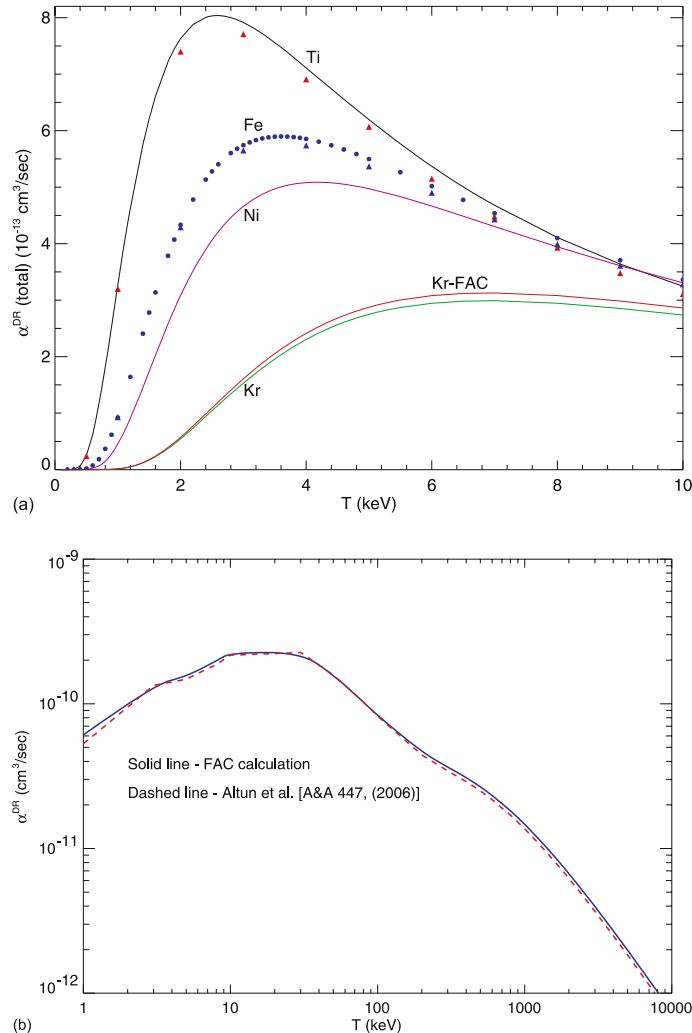


**Figure 2.** (a) total dielectronic recombination rate coefficients for He-like ions. Also shown are the scaled rate coefficients for Fe XXV (solid circles). The solid triangles are the results of Chen (1986a). DR rates for Kr using Cowan's code and FAC are in good agreement. (b) dielectronic recombination rates from ground state of Fe XVI. Solid line is FAC calculations and dashed line is calculations of Altun *et al.* (2006).

CC, also known as “R-matrix” (see Berrington *et al.* 1978), entails a full integration of the Schrödinger (or Dirac) equation for the electron + target system. Resonances are included naturally so long as coupling to the resonant states is included in the wavefunction expansion. Resonances must be included “by hand” in DW approaches. Not being based on perturbation theory, R-matrix approach is suitable for less highly charged ions, but at the expense of a large increase in computation time.

We focus our investigations in calculating dielectronic recombination rates since calculations of M-shell DR rates pose major challenges due to the complexities involved

in handling the complex atomic structures of large number of excited levels for these ions. Especially relevant is the determination of charge states of ions  $\text{Fe}^{8+}$ – $\text{Fe}^{12+}$  observed in the solar wind environment. These are important in CME cavities where Fe recombines to  $\text{Fe}^{8+}$  and beyond. In the fast solar wind  $\text{Fe}^{8+}$ – $\text{Fe}^{12+}$  represent the dominant Fe charge states. Although there exist a series of DR data for dynamic finite-density plasmas of L-shell ions, this is not appropriate for higher temperature Fe plasmas in the solar wind and detailed and accurate calculations must be performed for reliability. However, a recent calculation by Badnell (Badnell 2006) reports high temperature DR rate coefficients for M-shell Fe ions.

Most published work based on simple formula of Burgess (1965) and other detailed calculations give only Maxwellian averaged DR rate coefficients and not DR cross sections. For studying events in the solar wind, it is extremely important to have the cross sections which can be averaged over any relevant electron distribution to generate the rates. Unfortunately there is very little to almost none of these cross sections that are available in the literature, and in their calculations of ionization balance, Laming & Lepri (2007) had to simulate rates integrated over a kappa distribution by an appropriate sum over several Maxwellian averaged rates. Maxwellian averaged rate coefficients for dielectronic recombination of course facilitate comparisons with other published work.

In Fig. 2(a), we show a comparison of DR rate coefficients of several Li-like ions obtained using Cowan's code. Detailed calculations were carried out for a few ions and then scaling laws were developed to generate data for other ions in the isoelectronic sequence. We show a comparison of DR rates obtained using Cowan's code and FAC for Kr XXXIV. FAC results agree very well with those obtained using Cowan's code.

In Fig. 2(b), we show the DR rate coefficient for Fe XVI for a wide range of temperature obtained using FAC and compare them with those obtained by Altun *et al.* (2006) using the AUTOSTRUCTURE code. In FAC, DR data are calculated in the independent-process, isolated resonance approximation. In this calculation,  $\Delta N = 0$  channels that contribute mainly and significantly to the low-temperature DR rates are included along with the  $\Delta N = 1$  excitations. Both  $\Delta N = 0$  and  $\Delta N = 1$  DR resonances of Fe XVI were measured in storage-ring experiments by Linkemann *et al.* (1995). We can compare our resonance strengths with their data by convolving with the experimental energy resolution.

Very good agreement of our previous calculations of DR rates for a number of ions with the results of complex multi-configuration fully-relativistic results of Chen for Ar through Mo, and the sample DR calculation of M-shell Fe XVI using FAC, gives us extreme confidence in obtaining accurate DR rates Fe for all the M-shell ionization stages of concern.

## References

- Altun, Z., Yumak, A., Badnell, N. R., Loch, S. D., Pindzola, M. S. 2006, *Astron. Astrophys.*, **447**, 1165.
- Badnell, N. R. 2006, *Astrophys. J.*, **651**, L73.
- Berrington, K. A., Burke, P. G., Le Dourneuf, M., Robb, W. D., Taylor, K. T., Ky Lan, Vo 1978, *Computer Physics Commununcions*, **14**, 367.
- Bryans, P., Badnell, N. R., Gorczyca, T. W., Laming, J. M., Mitthumsiri, W., Savin, D. W. 2006, *Astrophys. J. Suppl.*, **167**, 343.

- Burgess, A. 1965, *Astrophys. J.*, **141**, 1589.
- Dasgupta, A., Whitney, K. G. 2004, *Phys. Rev. A.*, **69**, 022702.
- Laming, J. M. 2004, *Astrophys. J.*, **604**, 874.
- Laming, J. M., Lepri, S. T. 2007, *Astrophys. J.*, **660**, 1642.
- Linkemann, J., Müller, A., Kenntner, J., Habs, D., Schwalm, D., Wolf, A., Badnell, N. R., Pindzola, M. S. 1995, *Phys. Rev. Lett.*, **74**, 4173.
- Mazzotta, P., Mazzitelli, G., Colafrancesco, S., Vittorio, N. 1998, *Astron. Astrophys. Suppl.*, **133**, 403.
- Nahar, S. N. 1999, *Astrophys. J. Suppl.*, **120**, 131.